Energy Engineering

Tech Science Press

DOI: 10.32604/EE.2021.017270

ARTICLE

Modelling and Optimal Design of Hybrid Power System Photovoltaic/Solid Oxide Fuel Cell for a Mediterranean City

Bachir Melzi[1], Nesrine Kefif[2], Mamdouh El Haj Assad[3,*], Haleh Delnava[4] and Abdulkadir Hamid[5]

[1]School of Materials Sciences and Engineering, Wuhan University of Technology, Wuhan, China
[2]Power and Control Department, Electronic and Electrical Engineering Institute, M'hamed Bougara University, Boumerdes, Algeria
[3]Sustainable and Renewable Energy Engineering Department, University of Sharjah, Sharjah, United Arab Emirates
[4]Institute of Manufacturing Information and Systems, National Cheng Kung University, Tainan, Taiwan
[5]Electrical Engineering Department, University of Sharjah, Sharjah, United Arab Emirates
*Corresponding Author: Mamdouh El Haj Assad. Email: massad@sharjah.ac.ae

Received: 27 April 2021 Accepted: 03 August 2021

ABSTRACT

This work presents a hybrid power system consisting of photovoltaic and solid oxide fuel cell (PV-SOFC) for electricity production and hydrogen production. The simulation of this hybrid system is adjusted for Bou-Zedjar city in north Algeria. Homer software was used for this simulation to calculate the power output and the total net present cost. The method used depends on the annual average monthly values of clearness index and radiation for which the energy contributions are determined for each component of PV/SOFC hybrid system. The economic study is more important criterion in the proposed hybrid system, and the results show that the cost is very suitable for the use of this hybrid system, which ensures that the area is fed continuously with the sufficient energy for the load which assumed to be 500 kW in the peak season. The optimized results of the present study show that the photovoltaic is capable of generating 8733 kW electricity while the SOFC produces 500 kW electricity. The electrolyzer is capable of producing 238750 kg of hydrogen which is used as fuel in the SOFC to compensate the energy lack in nights and during peak season.

KEYWORDS

Energy storage; PV/SOFC; hybrid systems; hydrogen production; energy and economic optimization

1 Introduction

For sustainable development, the transmission of electrical energy for isolated areas is problematic and it occurs at high cost. Therefore, using renewable energy sources is imperative. For the increase of system reliability and security, a hybrid energy source schemes should be adopted [1]. Several works have discussed how to determine the optimal design of hybrid energy systems, where it results that separated renewable energy hybrid generation systems proved itself as a good solution for isolated areas or where a lack of grid is faced [2]. There are many works about design and analyses in the context of hybrid renewable energy power generation [3,4] where the results

were very promising. For this reason, it is advisable to think about PV/SOFC hybrid system in the region of Bou-Zedjar in the north of Algeria due to its favorable climate, which is suitable for PV operating temperature. In fact, this advanced technology can be used on a large scale [5–8]. Additionally, a battery storage is required [9–11] to ensure the continuous source of electricity. The use of super capacitors in the case of energy storage problems is a viable solution [12,13]. The complementary combination of renewable energy sources provides a continuous power output with the support of storage devices hence the hybrid system is more reliable [14,15].

The application of the proposed hybrid system is a challenging and important step as Algeria has strong solar energy capabilities, and it needs to develop systems with renewable energy sources for the large number of remote areas in the country. Therefore, it is necessary to know the contribution of each source (PV/SOFC) to provide the required electricity load to produce, taking into account the economic factor. In case the renewable sources are unable to handle the load demand, the hybrid system can be supported with a conventional energy source such as diesel generator [16–21].

According to reviews of other research works, the present study was not only able to meet the energy needs of the region by proposing the following hybrid system (PV/SOFC), but also reduce the initial cost. Based on this optimization, the proposed system can be used for replacing diesel generators and reducing the polluting gases. The most important point in this research is that the optimization of the system is considered without using the battery for energy storage, which has a significant effect on the cost. According to the authors knowledge, this study is the first work that has been applied to a city in Algeria.

2 Literature Review

Renewable energy sources became a good solution for many home owners in the world for the reduction of grid dependency, and thus a big domain of study for researchers; a case study in Sapporo, Japan where the energy consumption reduced by 66% for residents with PV/Fuel Cell (FC) energy system [22], as well as for rural areas, the off-grid applications are essential for farms in water pumping, or small villages, as the case of Northern Australia where Solar/Metal Hydride/Fuel Cell became the energy source for more than 100 communities with a load of hundreds of kW [23], in some studies, the real and reactive power (PQ) in a PV/SOFC microgrid operation was controlled for load changes in a grid connected and islanded mode for maximizing the power output using a heuristic method (artificial bee colony (ABC)) [24], or using fuzzy logic controller (FLC) for the Maximum Power Point Tracker (MPPT) purpose in solar power for a PV/SOFC system by considering a 1.26 kW proton exchange membrane FC with 950 W PV power output [25]. "V. P. Vinod" used the Improved Particle Swarm Optimization (IPSO) for the control of the voltage and frequency of the PV/SOFC microgrid [26]. A study case combined tidal power with PV/SOFC system in Ternate and Pulau-Tidore Islands with a maximum load of 1200 kW, a battery Energy Storage System (BESS) also has been added for better reliability with a 38.6 kWh storage capacity [27]; and a comparison of PV/BESS with PV/SOFC technologies ended with showing the preference of the PV/SOFC system which has lower cost and better feasibility, such that for 25 years of work, the Levelized cost of electricity (LCOE) for PV/BESS is 0.16 US$/kWh, and 0.11 US$/kWh for PV/SOFC [28].

3 Area Presentation

The chosen site for our study is an isolated coastal and tourist village in Algeria called Bou-Zedjar at latitude: 35.5744°N and longitude: −1.16695°E. This village is located in Ain

Temouchent province and consists of a few tourist complexes. The actual readings for the location were obtained from the NASA atmospheric data center [29]. Solar PV and SOFC can be a sustainable and more convenient solution for providing environmentally friendly energy. Meteorological data used are solar radiation and ambient temperature for this area.

4 Homer Software

Hybrid Optimization Model for Electric Renewables (HOMER) is a computer software which is developed by the U. S. National Renewable Energy Laboratory to make the hybrid power configuration systems easier as well as their technology comparison in different designs [30].

The simulation covers a study period of one year with 1 min step, which analyzes the design sensitivity and gives outputs to different inputs before the design construction. The optimization simulation goal is the economic evaluation and technical possibility in terms of technology, cost and energy resource availability [30–34].

The software simulation gives several possible designs, with a best hybrid power system configuration optimization [35]. In this study, different options such: PV generators, fuel cells, electrolyzer, and a hydrogen storage as a hybrid power system were used.

The annual assessment of the climatic characteristics of the site is shown in Fig. 1 and Tab. 1.

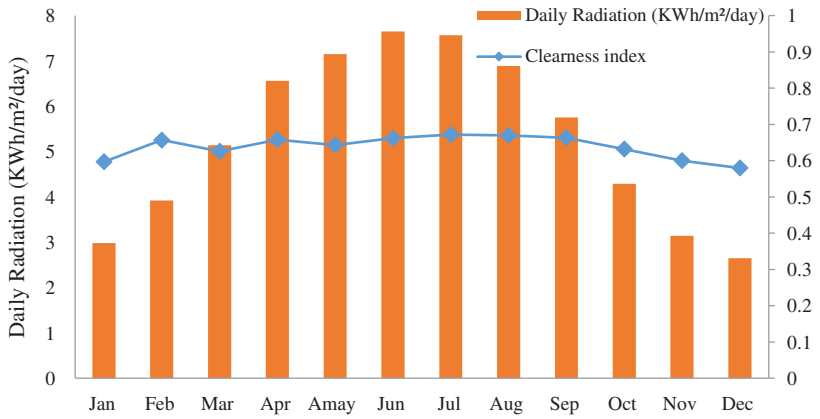

Figure 1: Daily Radiation (kWh/m^2/day) and clearness index

Fig. 1 shows that the Bou-Zedjar City has a good amount of solar radiation throughout the year, especially in summer. It can be observed from Tab. 1 that the clearness index is in the range of 0.58 to 0.7, which means that clean energy can be generated with high return. Thus, a hybrid power system consisting of a PV/SOFC is a viable strategy and a feasible solution.

Table 1: Monthly average solar global horizontal irradiance (GHI) data

Month	Clearness index	Daily radiation (kWh/m^2/day)
January	0.597	2.980
February	0.617	3.920
March	0.626	5.140
April	0.658	6.560
May	0.643	7.150
June	0.662	7.650
July	0.672	7.570
August	0.670	6.890
September	0.663	5.750
October	0.632	4.290
November	0.600	3.140
December	0.580	2.650

4.1 Mathematical Formulations

The mathematical formulations of the prosed hybrid system are given in the next sections and these formulations are solved in order by HOMER software.

4.1.1 Clearness Index

The monthly average clearness index is defined as:

$$K_T = \frac{H_{ave}}{H_{o,ave}} \tag{1}$$

where H_{ave} is the monthly average radiation on the horizontal surface of the earth [kWh/m^2/day] and $H_{o,ave}$ is the extraterrestrial horizontal radiation, meaning the radiation on a horizontal surface at the top of the earth's atmosphere [kWh/m^2/day].

$H_{o,ave}$ can calculated for any month of the year for a given latitude. By knowing either H_{ave} or K_T, HOMER is able to compute the other for each new value entered into the monthly data table in the solar resource inputs using Eq. (1).

The following equation is used by HOMER to calculate the intensity of solar radiation at the top of the Earth's atmosphere:

$$G_{on} = G_{sc}\left(1 + 0.033.\cos\frac{360n}{365}\right) \tag{2}$$

where G_{sc} is the solar constant which is considered as 1.367 kW/m^2 and n is the day of the year [30].

Eq. (2) gives the extraterrestrial radiation on a surface normal to the sun's rays.

The extraterrestrial radiation on the horizontal surface is expressed by:

$$G_o = G_{on}\cos\theta_Z \tag{3}$$

where θ_Z is the zenith angle which is calculated from:

$$\cos\theta_Z = \cos\emptyset\cos\delta\cos\omega + \sin\emptyset\sin\delta \tag{4}$$

where ϕ is the latitude, δ is the solar declination angle and ω is the hour angle.

The solar declination angle is expressed by:

$$\delta = 23.45^{\circ}\sin\left(360^{\circ}\frac{284+n}{365}\right) \tag{5}$$

where n is the day of the year.

The total daily extraterrestrial radiation per square meter can be found by computing the integral of G_o from sunrise to sunset. The following equation is built after integration:

$$H_o = \frac{24}{\pi}\ G_{on}\left[\cos\emptyset\ \cos\delta\sin\omega_s + \frac{\pi\omega_s}{180^{\circ}}\sin\emptyset\sin\delta\right] \tag{6}$$

where ω_s is the sunset hour angle which is calculated using the following equation:

$$\cos\omega_s = -\tan\emptyset\tan\delta \tag{7}$$

The average for the month using the following equation:

$$H_{o,ave} = \frac{\sum_{n=1}^{N} H_0}{N} \tag{8}$$

where N is the number of days in the month.

HOMER software divides the monthly average global solar radiation by $H_{o,ave}$ to find the monthly average clearness index.

4.1.2 Radiation Incident on PV Array

The location of the sun in the sky depends on the time of day, it can be described by an hour angle. HOMER takes the hour angle as zero at solar noon (when the position of the sun is in the highest point in the sky), negative before solar noon, and positive after solar noon. The hour angle can be found using the following equation:

$$\omega = (t_s - 12hr)\cdot 15 \tag{9}$$

where t_s is the solar time in hours.

It is assumed that all time-dependent data are specified in civil time (local standard time) not in solar time. The solar time in hours is calculated by:

$$t_s = t_c + \frac{\lambda}{15^{\circ}/hr} - Z_c + E \tag{10}$$

where t_c is the civil time in hours corresponding to the midpoint of the time step [hr], λ is the longitude [°], Z_c is the time zone in hours east of GMT [hr] and E is the equation of time [hr]

The equation of time is calculated as:

$$E = 3.82(0.000075 + 0.001868\cdot\cos B - 0.032077\cdot\sin B - 0.014615\cdot\cos 2B - 0.04089\cdot\sin 2B) \tag{11}$$

where B is given by:

$$B = 360^{\circ}\frac{(n-1)}{365} \tag{12}$$

where n is the day of the year, starting on the first of January.

The angle of incidence can be defined using the following equation:

$$\cos\theta = \sin\delta\sin\phi\cos\beta - \sin\delta\cos\phi\sin\beta\cos\gamma + \cos\delta\cos\phi\cos\beta\cos\omega + \cos\delta\sin\phi\sin\beta\cos\gamma\cos\omega + \cos\delta\sin\beta\sin\gamma\sin\omega \tag{13}$$

where θ is the angle of incidence, β the surface slope, γ is the azimuth of the surface.

Because of the simulation on a time-step-by-time-step basis in HOMER software, the equation of the extraterrestrial radiation on the horizontal surface is integrated over one time step to find the average extraterrestrial horizontal radiation over the time step:

$$\overline{G_o} = \frac{12}{\pi}G_{on}\left[\cos\phi\cos\delta(\sin\omega_2 - \sin\omega_1) + \frac{\pi(\omega_2-\omega_1)}{180^{\circ}}\sin\phi\sin\delta\right] \tag{14}$$

where ω_1 is the hour angle at the beginning of the time step and ω_2 is the hour angle at the end of the time step.

The clearness index is defined as follows:

$$k_T = \frac{\bar{G}}{\bar{G}_o} \tag{15}$$

where $\bar{G}$ is the global horizontal radiation on the earth's surface averaged over the time step. The global solar radiation is expressed by the following equation:

$$\overline{G} = \overline{G_b} + \overline{G_d} \tag{16}$$

where G_b is the beam radiation and G_d is the diffuse radiation.

HOMER measures only the global horizontal radiation in most cases that is why HOMER's Solar Resource Inputs should be filled up with the global horizontal radiation then, in every time step, HOMER will find its components to define the radiation incident on the PV array. The diffuse fraction as a function of the clearness index is expressed as [36]:

$$\frac{\bar{G}_d}{\bar{G}} = \begin{Bmatrix} 1.0 - 0.09\cdot k_T; & for: \ k_T \le 0.22 \\ 0.9511 - 0.1604\cdot k_T + 4.388\cdot k_T^2 + 16.638\cdot k_T^3 + 12.336\cdot k_T^4: & for: \ 0.22 < k_T \le 0.80 \\ 0.165; & for \ k_T > 0.80 \end{Bmatrix} \tag{17}$$

To calculate the global radiation striking the tilted surface of the PV array, HOMER uses the HDKR model (Hay & Davies, Klucher & Reindl) which assumes that there are three components of the diffuse solar radiation: an isotropic component, a circumsolar component, and a horizon brightening component.

The HDKR model calculates the global radiation incident on the PV array by the following equation:

$$\bar{G}_T = (\bar{G}_b + \bar{G}_d A_i) R_b + \bar{G}_d (1 - A_i) \left(\frac{1 + cos\,\beta}{2} \right) \left[1 + \sin^3 \left(\frac{\beta}{2} \right) \right] + \bar{G} \rho_g \left(\frac{1 - \cos \beta}{2} \right) \tag{18}$$

where A_i is the anisotropy index which is defined as $A_i = \frac{\bar{G}_b}{\bar{G}_o}$ and F is a factor defined as $f = \sqrt{\frac{\bar{G}_b}{\bar{G}}}$.

where ρ_g is the ground reflectance [%].

4.1.3 PV Array Power Output

The output of the PV array is obtained by:

$$P_{PV} = Y_{PV} f_{PV} \left(\frac{\bar{G}_T}{\bar{G}_{T,STC}} \right) [1 + \alpha_P (T_c - T_{c,STC})] \tag{19}$$

where Y_{PV} is the rated capacity of the PV array, meaning its power output under Standard Test Conditions (STC) [kW], f_{PV} is the PV derating factor [%], $\bar{G}_T$ is the solar radiation incident on the PV array in the current time step [kW/m^2], $\bar{G}_{T,STC}$ is the incident radiation at STC [1 kW/m^2], α_P is the temperature coefficient of power [%/°C], T_c is the PV cell temperature in the current time step [°C] and $T_{c,STC}$= the PV cell temperature under STC [25°C].

5 System Presentation

5.1 Hybrid System Modeling

The proposed hybrid system consists of two energy providers: photovoltaic cells (PV) and solid oxide fuel cell (SOFC); in addition to an electrolyzer to provide hydrogen which is stored in a hydrogen tank and a converter. Fig. 2 shows the schematic of PV/SOFC hybrid system.

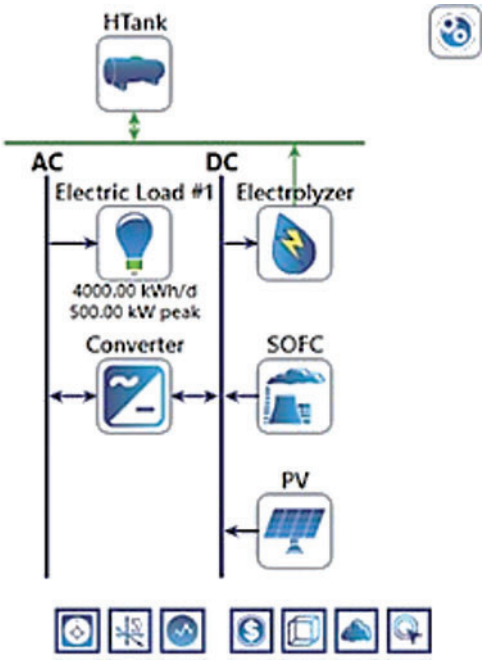

Figure 2: Schematic of the proposed PV/SOFC hybrid system

5.2 Electrical Load Profile

Fig. 3 shows the variations of hourly average load for all months of the year. it is noted that there is a difference in the annual peak load between winter and summer seasons, where the highest value was recorded in June to July with 500 KW, while the lowest value of load was recorded in the fall and winter season (November to January) with 160 kW.

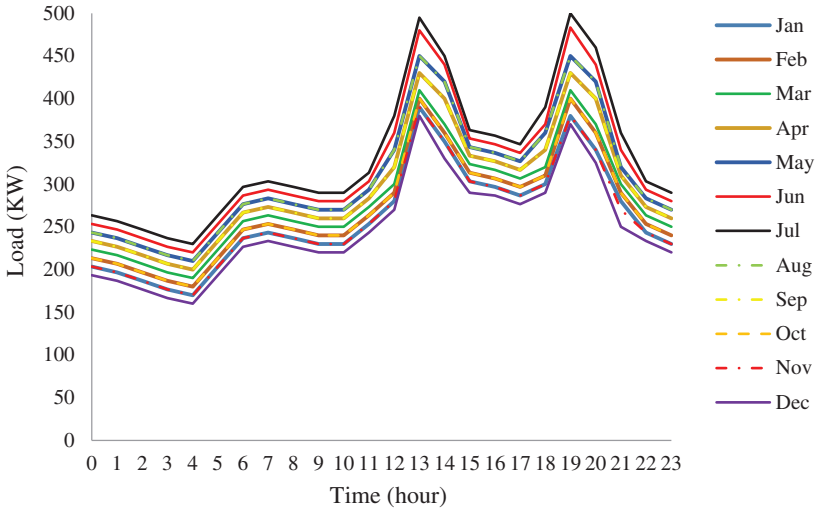

Figure 3: Hourly average load variations in a year for all months

The annual operation output divided by the load is shown in Fig. 4, while Fig. 5 shows the annual operation output divided by the generator load.

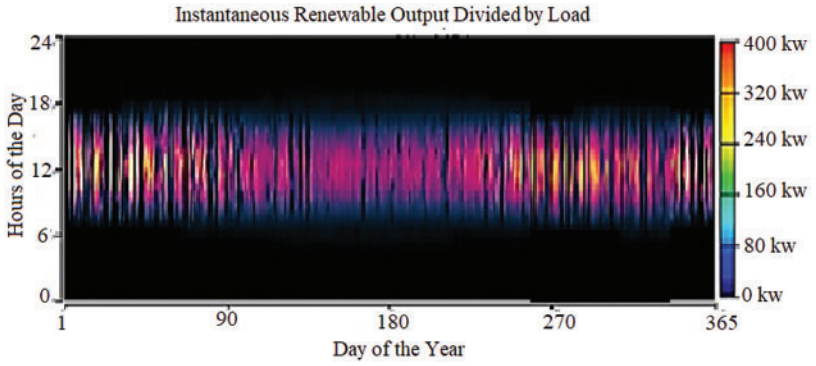

Figure 4: Instantaneous renewable output divided by load

The annual operation outputs of the SOFC and PV are shown in Figs. 6a and 6b, respectively. According to the weather data and the load demand of Bou-Zedjar City, we used the results presented in Figs. 4–6, to understand the operational strategy for our power hybrid system.

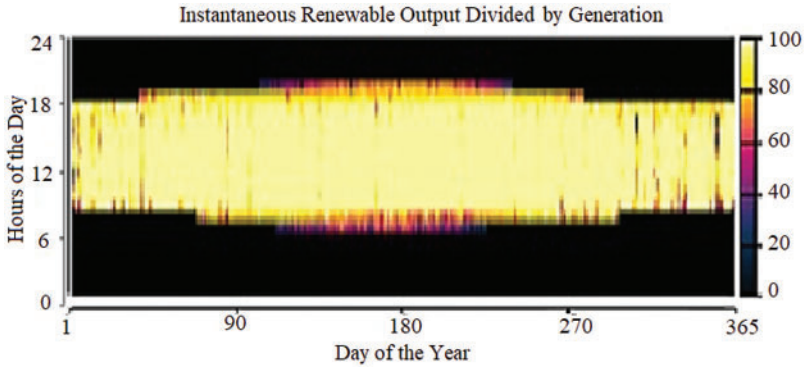

Figure 5: Instantaneous renewable output divided by generation

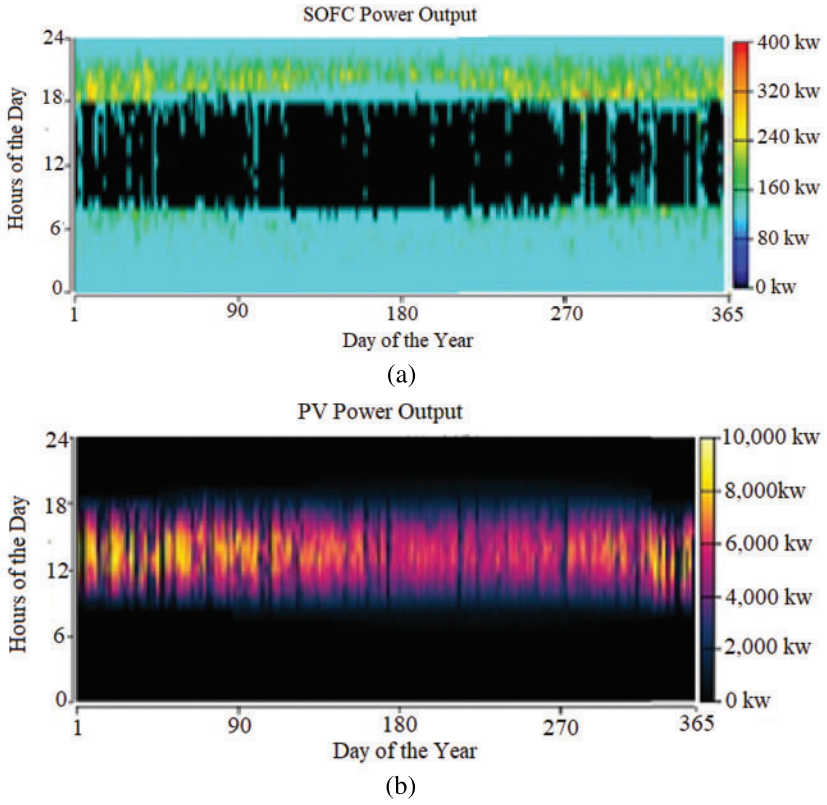

Figure 6: (a) The SOFC power output; (b) The PV power output

6 Solar Resource with PV and SOFC Generator Data

Since the PV cells produce direct current, a converter is used to convert the direct current produced by the photovoltaic cells into alternating current. The solar cells will produce water vapor which is sent to the electrolyzer whose function is to separate the hydrogen gas and send it for storage in the storage tank. The stored hydrogen is used by the SOFC which is for energy compensation when the sun is unavailable (night and rainy days).

The energy produced by the two generators is shown in Fig. 7.

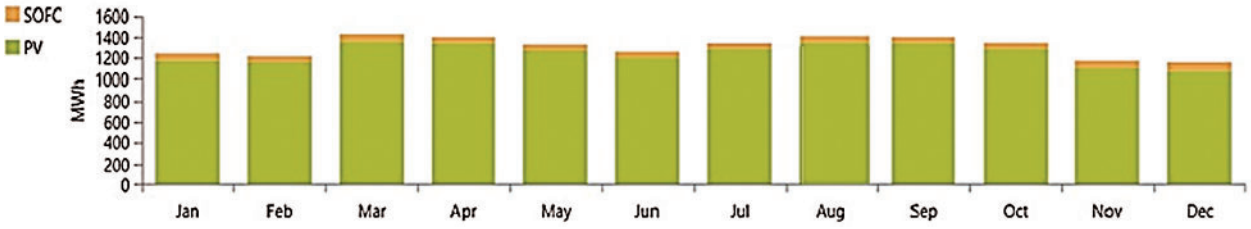

Figure 7: The energy produced by the PV and SOFC generators

Since the load demand of the chosen region varies throughout the year, and so the weather data, the PV and SOFC are going to work in a variable way; the fuel consumption is shown in Fig. 8. Thus, the power produced by the stored hydrogen also will vary throughout the year as shown in Fig. 9.

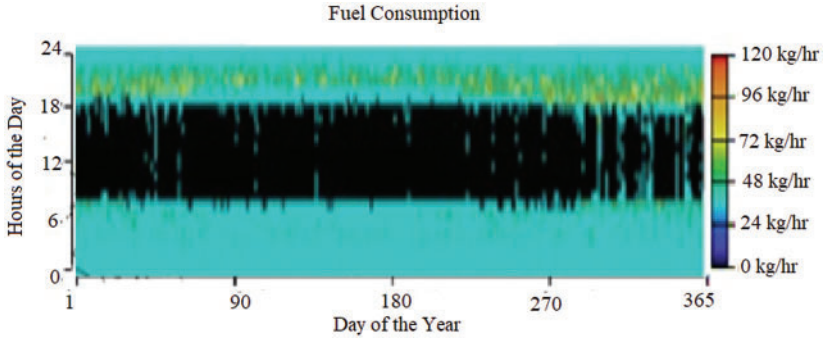

Figure 8: Fuel consumption

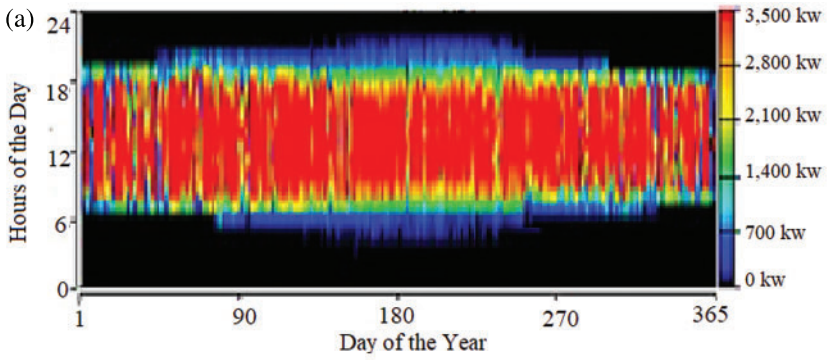

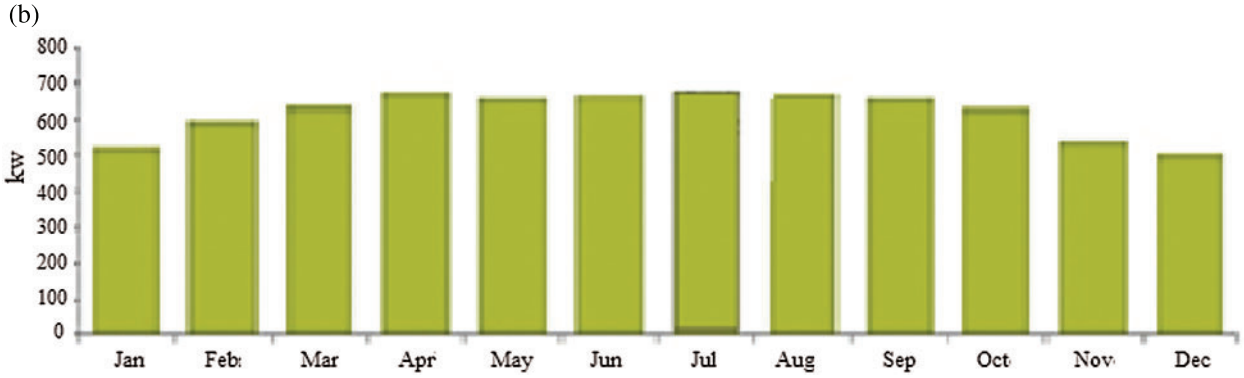

Figure 9: (a) Electrolyzer output power; (b) Electrolyzer input power

7 Optimized Results

After the simulation process with Homer software, in which climate data for Bou-Zedjar region were used and an annual clearness index of 0.643, and considering the capacities of different hybrid system options: (PV, fuel cell, electrolyzer, hydrogen storage), the capacities are obtained and presented in Tab. 2.

Table 2: Optimization results

PV (kW)	8,733
SOFC (kW)	500
Converter (kW)	459
Electrolyzer (kW)	3,500
Storage tank of H_2 (kg)	238,750
Capital cost ($)	2,484,235
Total cost of hybrid power system ($)	3,266,865
Cost of energy ($/kWh)	0.173
Operating cost ($/yr)	60,540

Fig. 10 and Tabs. 2 and 4 summarize the HOMER-based optimization of the FC/PV hybrid system, the Total Net Present Cost (TNPC) is 3, 266,865,64$ with a capital cost of 3,484,235,96$.

Tab. 3 shows the hybrid power system annual emissions, where the monoxide emission is below zero because our system is a carbon negative since it removes more than the emitted carbon into the atmosphere.

The constructed system should supply the power required by Bou-Zedjar city as well as satisfying its yearly load with an annual real interest rate of 0.2%.

For a hybrid system lifetime of 25 years:

The annual real interest rate = the nominal interest rate − the inflation rate.

The input data to HOMER software are shown in Tab. 5 [37,38].

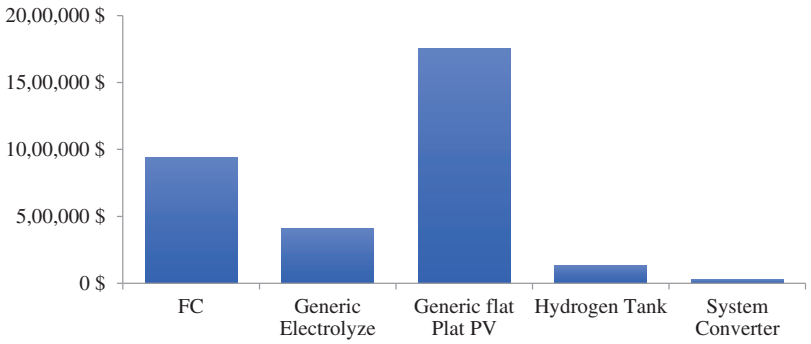

Figure 10: Cost summary of fuel cell (FC), generic electrolyzer, generic flat plate PV, hydrogen tank and System converter

Table 3: Annual emissions of the hybrid system

Component	Value (kg/yr)
CO_2	−4,800
CO	3,055
Unburned Hydrocarbons	162
Other Nano-particulate	26.1
Nitrogen Oxides	585

Table 4: The cost of the system and its components

Component	Capital ($)	Replacement ($)	O & M ($)	Salvage ($)	Total ($)
FC	250,000,00	163,130,52	562,502,10	35,155,11	940,477,50
Generic electrolyzer	350,000,00	14,849,58	45,264,31	52,794,84	407,301,05
Generic flat plate PV	1,74651537	0.00	5,644,53	0.00	1,752,159,90
Hydrogen tank	119,375,00	3,805,76	15,432,22	2,144,79	136,468,19
System converter	18,345,59	584,87	11,858,14	329,61	30,458,99
System	3,484,235,96	182,370,73	640,638,30	40,424,36	3,266,865,64

Table 5: Input data cost/option

Options	Cost			
	The Capital ($)	Replacement ($)	Operations & Maintenance ($/year)	Life (year)
P-V	20,000/100 kW	20,000	5	25
SOFC	2,500/5 kW	2,000	0.1 (Cost/h/kw)	6.86
Converter	4,000/100 kW	200	100	20
H_2	500/5 kW	50	10	15
Electrolyzer	2,000/20 kW	100	10	15

8 Conclusion

In this paper, the optimal design of PV/FC hybrid power system has been studied to meet the load demand of Bou-Zedjar City, Ain Temouchent in Algeria without the need for a battery storage. The PV panels can provide enough energy to feed the load with an extra energy used to produce the hydrogen for SOFC for power generation later in night or in cloudy days where the FC generator is a guaranteed compensator for satisfying the growing loads that are assumed to be 500 kW in the peak season. The optimization process revealed that the PV was capable of producing 8.733 MW, the SOFC generated 0.5 MW, and the electrolyzer produced 238570 kg of hydrogen with a total cost of the hybrid power system of 3,266,865$.

The results insured the ability of the fuel cell generator to provide the necessary growing loads, as well as its ability to be a renewable source of energy. In addition to be a non-polluting reliable energy source, the study of economic performance using HOMER software has proved that the previous PV/SOFC hybrid power system is a suitable combination with the ability to replace the diesel generators in addition of being less expensive in maintenance.

Funding Statement: The authors received no specific funding for this study.

Conflicts of Interest: The authors declare that they have no conflicts of interest to report regarding the present study.

References

1. Mohammed, O. H., Amirat, Y., Benbouzid, M. E. H., Tang, T. (2013). Hybrid generation systems planning expansion forecast: A critical state of the art review. *Proceeding of the 2013 IEEE IECON*, pp. 1666–1671. Vienna, Austria.
2. Markvart, T. (1996). Sizing of hybrid photovoltaic-wind energy systems solar energy. *Solar Energy, 57(4),* 277–281. DOI 10.1016/S0038-092X(96)00106-5.
3. Alam, M. S., Gao, D. W. (2006). Design modeling analysis of a hybrid wind, fuel cell distributed generation system for stand-alone applications. *Global Conference on Renewable Energy Approaches for Desert Regions*, pp. 22. Amman, Jordan.
4. Onar, O. C., Uzunoglu, M., Alam, M. S. (2006). Dynamic modeling, design and simulation of a wind/fuel cell/ultra-capacitor-based hybrid power generation system. *Journal of Power Sources, 161(1),* 707–722. DOI 10.1016/j.jpowsour.2006.03.055.
5. Abanda, F. H., Tah, J. H. M., Duce, D. (2013). PV-Tons: A photovoltaic technology ontology system for the design of PV-systems. *Engineering Applications of Artificial Intelligence, 26(4),* 1399–1412. DOI 10.1016/j.engappai.2012.10.010.
6. Liu, Y. H., Liu, C. L., Huang, J. W., Chen, J. H. (2013). Neural-network-based maximum power point tracking methods for photovoltaic systems operating under fast changing environments. *Solar Energy, 89,* 42–53. DOI 10.1016/j.solener.2012.11.017.
7. Himour, K., Ghedamsi, K., Berkouk, E. M. (2014). Supervision and control of grid connected PV-storage systems with the five level diode clamped inverter. *Energy Conversion and Management, 77,* 98–107. DOI 10.1016/j.enconman.2013.09.001.
8. Lizin, S., van Passel, S., de Schepper, E., Vranken, L. (2012). The future of organic photovoltaic solar cells as a direct power source for consumer electronics. *Solar Energy Materials and Solar Cells, 103,* 1–10. DOI 10.1016/j.solmat.2012.04.001.
9. Semaoui, S., Arab, A. H., Bacha, S., Azoui, B. (2013). Optimal sizing of a stand-alone photovoltaic system with energy management in isolated areas. *Energy Procedia, 36,* 358–368. DOI 10.1016/j.egypro.2013.07.041.

10. Ru, Y., Kleissl, J., Martinez, S. (2014). Exact sizing of battery capacity for photovoltaic systems. *European Journal of Control, 20(1),* 24–37. DOI 10.1016/j.ejcon.2013.08.002.
11. Semaoui, S., Hadj Arab, A., Bacha, S., Azoui, B. (2013). The new strategy of energy management for a photovoltaic system without extra intended for remote-housing. *Solar Energy, 94,* 71–85 DOI 10.1016/j.solener.2013.04.029.
12. Li, J., Chen, Y., Liu, Y. (2012). Research on a stand-alone photovoltaic system with a supercapacitor as the energy storage device. *Energy Procedia, 16,* 1693–1700. DOI 10.1016/j.egypro.2012.01.262.
13. Glavin, M. E., Chan, P. K. W., Armstrong, S., Hurley, W. G. (2008). A stand-alone photovoltaic supercapacitor battery hybrid energy storage system. *2008 13th International Power Electronics and Motion Control Conference*. Poznan, Poland.
14. Hiendro, A., Kurnianto, R., Rajagukguk, M., Simanjuntak, Y. M., Junaidi (2013). Techno-economic analysis of photovoltaic/wind hybrid system for onshore/remote area in Indonesia. *Energy, 59,* 652–657. DOI 10.1016/j.energy.2013.06.005.
15. Kabalci, E. (2013). Design and analysis of a hybrid renewable energy plant with solar and wind power. *Energy Conversion and Management, 72,* 51–59. DOI 10.1016/j.enconman.2012.08.027.
16. Merei, G., Berger, C., Sauer, D. U. (2013). Optimization of an off-grid hybrid PV–Wind–Diesel system with different battery technologies using genetic algorithm. *Solar Energy, 97,* 460–473. DOI 10.1016/j.solener.2013.08.016.
17. Colantoni, A., Allegrini, E., Boubaker, K., Longo, L., di Giacinto, S. et al. (2013). New insights for renewable energy hybrid photovoltaic/wind installations in Tunisia through a mathematical model. *Energy Conversion and Management, 75,* 398–401. DOI 10.1016/j.enconman.2013.06.023.
18. Kumar, R., Gupta, R. A., Bansal, A. K. (2013). Economic analysis and power management of a stand-alone wind/photovoltaic hybrid energy system using biogeography based optimization algorithm. *Swarm and Evolutionary Computation, 8,* 33–43. DOI 10.1016/j.swevo.2012.08.002.
19. Boudries, R. (2013). Analysis of solar hydrogen production in Algeria: Case of an electrolyzer-concentrating photovoltaic system. *International Journal of Hydrogen Energy, 38(26),* 11507–11518. DOI 10.1016/j.ijhydene.2013.04.136.
20. Rekioua, D., Bensmail, S., Bettar, N. (2014). Development of hybrid photovoltaic-fuel cell system for stand-alone application. *International Journal of Hydrogen Energy, 39(3),* 1604–1611 DOI 10.1016/j.ijhydene.2013.03.040.
21. Chávez-Ramírez, A. U., Vallejo-Becerra, V., Cruz, J. C., Ornelas, R., Orozco G. et al. (2013). A hybrid power plant (Solar–Wind–Hydrogen) model based in artificial intelligence for a remote-housing application in Mexico. *International Journal of Hydrogen Energy, 38(6),* 2641–2655. DOI 10.1016/j.ijhydene.2012.11.140.
22. Hamada, Y., Takeda, K., Goto, R., Kubota, H. (2011). Hybrid utilization of renewable energy and fuel cells for residential energy systems. *Energy and Buildings, 43(12),* 3680–3684. DOI 10.1016/j.enbuild.2011.09.042.
23. Gray, E. M., Webb, C. J., Andrews, J., Shabani, B., Tsai, P. J. et al. (2011). Hydrogen storage for off-grid power supply. *International Journal of Hydrogen Energy, 36(1),* 654–663. DOI 10.1016/j.ijhydene.2010.09.051.
24. Bai, W., Abedi, M. R., Lee, K. Y. (2016). Distributed generation system control strategies with PV and fuel cell in microgrid operation. *Control Engineering Practice, 53,* 184–193. DOI 10.1016/j.conengprac.2016.02.002.
25. Jyotheeswara Reddy K., Sudhakar N. (2018). Design and analysis of a hybrid PV-PEMFC system with MPPT controller for a three-phase grid-connected system. *Journal of Green Engineering, 8(2),* 151–176. DOI 10.13052/jge1904-4720.823.
26. Prabhakaran, V. V., Singh, A. (2019). Enhancing power quality in PV-SOFC microgrids using improved particle swarm optimization. *Journal of Engineering, Technology & Applied Science Research, 9(5)*. DOI 10.48084/etasr.2963.

27. Siti Khodijah, A., Shiba, M., Obara, S. (2020). Design of compensation battery for tidal power-photovoltaics-SOFC microgrids in Ternate and Pulau-Tidore islands. *International Journal of Energy*. DOI 10.1002/er.5904.
28. Al-Khori, K., Bicer, Y., Koç, M. (2021). Comparative techno-economic assessment of integrated PV-SOFC and PV-battery hybrid system for natural gas processing plants. *Journal of Energy, 222,* 119923. DOI 10.1016/j.energy.2021.119923.
29. Earth Data Website (2020). http://eosweb.larc.nasa.gov/sse/.
30. Homer Modeling Software (2019). http://homerenergy.com/.
31. Connolly, D. (2016). http://www.dconnolly.net/research/planning/tools/index.html.
32. Lambert, T., Gilman, P., Lilienthal, P. (2019). HOMER Modeling Information (software). http://www.pspb.org/e21/media/HOMERModelingInformation.pdf.
33. Lopez, N., Espiritu, J. F. (2011). An approach to hybrid power systems integration considering different renewable energy technologies. *Procedia Computer Science, 6,* 463–468. DOI 10.1016/j.procs.2011.08.086.
34. Markovic, D., Cvetkovic, D., Masic, B. (2011). Survey of software tools for energy efficiency in a community. *Renewable and Sustainable Energy Reviews, 15(9),* 4897–4903. DOI 10.1016/j.rser.2011.06.014.
35. Mohammed, O. H., Amirat, Y., Benbouzid, M., Elbaset, A. A. (2014). Optimal design of a PV/fuel cell hybrid power system for the city of brest in France. *2014 First International Conference on Green Energy* Sfax, Tunisia.
36. Erbs, D. G., Klein, S. A., Duffie, J. A. (1982). Estimation of the diffuse radiation fraction for hourly, daily and monthly-average global radiation. *Solar Energy, 28(4),* 293–302. DOI 10.1016/0038-092x(82)90302-4.
37. Karakoulidis, K., Mavridis, K., Bandekas, D. V., Adoniadis, P., Potolias, C. et al. (2011). Techno-economic analysis of a stand-alone hybrid photovoltaic-diesel–battery-fuel cell power system. *Renewable Energy, 36(8),* 2238–2244. DOI 10.1016/j.renene.2010.12.003.
38. Beccali, M., Brunone, S., Cellura, M., Franzitta, V. (2008). Energy, economic and environmental analysis on RET-hydrogen systems in residential buildings. *Renewable Energy, 33(3),* 366–382. DOI 10.1016/j.renene.2007.03.013.